Photoionization of sodium atoms and electron scattering from ionized sodium

Arati Dasgupta and A. K. Bhatia
Atomic Physics Office, Laboratory for Astronomy and Solar Physics, NASA, Goddard Space Flight Center, Greenbelt, Maryland 20771
(Received 9 April 1984)

The polarized-orbital method [originally developed by A. Temkin, Phys. Rev. **107**, 1004 (1957)] is used to calculate the photoionization cross sections of sodium atoms, from threshold to about 60 eV. The polarized orbitals are calculated from Sternheimer's equation. The polarizability of Na^+ is found to be $1.0914a_0^3$, which is very close to the experimental value. The scattering equation is solved in the exchange, the exchange-adiabatic, and the polarized-orbital approximations. For consistency, both the bound-state and the continuum-state wave functions are obtained in the same approximation. In the calculation of these wave functions, all perturbed orbitals are taken into account in the direct polarization potential and only the perturbation of the very tightly bound $1s$ orbital is neglected in the exchange-polarization terms. The length form for the photoionization-cross-section formula is used and all terms are included in the photoionization matrix element. Our results are in good agreement with the many-body calculations of Chang and Kelly. However, no calculation to date, including this one, agrees well with experiment except at low energies. The phase shifts thus obtained for s, p, and d waves for the $e + Na^+$ system are used to calculate the differential cross sections; the phase shifts, as well as these cross sections, agree very well with other available results.

I. INTRODUCTION

Photoionization processes have useful applications in determining the temperature and population density of the astrophysical and laboratory plasmas, especially if the plasmas are not in thermal equilibrium. In the case of photoionization of a neutral atom, the final state is equivalent to electron scattering from a positive ion. The information from the scattering problem can be useful in understanding the processes occurring in the upper atmosphere and in the laboratory plasmas, for example, in gaining information about transport of electrons through ionized gases.

The polarized-orbital method (POM) developed originally by Temkin[1] has been applied extensively for scattering problems. It is here used to calculate the wave functions for the continuum electron in the final state and for the bound $3s$ electron of the sodium atom in the initial state. Since there is one electron outside the closed shells in the alkali-metal atoms, one finds this method extremely suitable for calculations of photoionization cross sections for these atoms. Another reason that this method is very useful for photoionization calculations is the fact that one can solve both the initial-state and the final-state wave functions from the same equation and thus improve them consistently. Throughout this paper, we refer to the total system as the atomic Na^+ core plus the valence $3s$ electron in the initial state and core plus the continuum electron in the final state.

The application of POM in the photoionization of lithium by Bhatia *et al.*[2] gave good results when used in as orthodox a manner as possible. Other polarized-orbital-like calculations[3] can be criticized[2] precisely because they apply the POM inconsistently (a discussion of this is given in Ref. 2).

We shall find that in spite of the fact that our results, like all other theoretical results, disagree with the experiment[4] except at low energies, the close agreement of this calculation with the detailed many-body perturbation calculation of Chang and Kelly[5] is very encouraging.

In this paper we not only present the photoionization cross sections but also the phase shifts and differential cross sections for the elastic scattering of electrons from the Na^+ ion. Theoretical results of electron scattering from positive ions are rare and the availability of experimental data even scarcer. We thus think that these results would be of help for future use. In Sec. II we give the formula for the photoionization cross section. Section III is devoted to deriving the equation for the initial bound state and the final continuum state for the outer electron in the POM. Numerical results and graphs concerning these two states have also been included in that section. In Sec. IV the photoionization matrix elements are discussed and the cross sections obtained in this calculation are presented there. These photoionization cross sections are also compared to other theoretical and experimental results in this section. Finally, conclusions are presented briefly in Sec. V.

II. THE FORMULA FOR THE PHOTOIONIZATION CROSS SECTION

The photoionization cross section[6] (in Rydberg units) for a transition from an initial state i to a final state f is given by

$$\sigma = 4\pi k \alpha a_0^2 \omega \left| \left\langle \psi_f \left| \sum_{j=1}^{N} z_j \right| \psi_i \right\rangle \right|^2 , \tag{2.1}$$

where ω is the energy of the incident photon and k the momentum of the outgoing electron. ψ_i and ψ_f are the initial- and final-state wave functions. α is the fine-structure constant and a_0 the Bohr radius.

The basic part of the calculation of the photoionization cross sections then consists of the calculation of the photoionization matrix element

$$M=\left\langle \psi_f \left| \sum_{j=1}^{N} z_j \right| \psi_i \right\rangle . \tag{2.2}$$

III. THE INITIAL AND FINAL STATES

The wave function for the total system both in the initial and the final state can be written as[1,2]

$$\psi_{i,f}^{A}=A\{v_{i,f}(1)[\psi_0(2,3,\ldots,N+1) +\psi^{\text{pol}}(1;2,3,\ldots,N+1)]\} , \tag{3.1}$$

where A is the antisymmetrization operator. $v_l(1)$, $l=i,f$, represents the wave function for the $3s$ electron in the initial and the continuum electron in the final state. We notice that the wave function ψ^{pol} representing the polarization of the core contains parametrically the coordinate of the "outer" electron. This dependence is expected considering the fact that polarization is caused by the interaction of the outer electron with the core electrons.

In the spirit of the POM (Ref. 1) $v_l(1)$ is then determined from the equation

$$\int Y_{L0}^{*}(\Omega_1)\chi_{1/2}(\sigma_1)\psi_0^{*}(2,\ldots,N+1)(H_{N+1}-E) \times\psi_l^{A}d\sigma_1\prod_{j=2}^{N+1}d^3r_j d\sigma_j=0, \quad l=i,f \tag{3.2}$$

where integrations are made over all spin and space coordinates except the radial coordinate r_1. The total Hamiltonian H_{N+1} of the system can be written as

$$H_{N+1}=H_N+H_1 , \tag{3.3}$$

where

$$H_N=-\sum_{i=2}^{N+1}\left[\nabla_i^2-\frac{2Z}{r_i}\right]+\sum_{i=2}^{N+1}\sum_{\substack{j=2\\ j\neq i}}^{N+1}\frac{2}{r_{ij}} , \tag{3.4}$$

and

$$H_1=-\nabla_1^2-\frac{2Z}{r_1}+\sum_{j=2}^{N+1}\frac{2}{r_{1j}} , \tag{3.5}$$

and Z is the nuclear charge. We note that subscript 1 refers to the outer electron. The energy E in Eq. (3.2) is given by

$$E=E_0+\epsilon_1 , \tag{3.6}$$

where E_0 is the ground-state energy of the atomic core and ϵ_1 represents the energy of the outer electron. The unperturbed wave function ψ_0 of the core then satisfies

$$H_N\psi_0=E_0\psi_0 . \tag{3.7}$$

If we use Eq. (3.7) in Eq. (3.2), we get

$$\int Y_{L0}^{*}(\Omega_1)\chi_{1/2}(\sigma_1)\psi_0^{*}(\bar{1})(H_1-\epsilon_1) \times\psi_l^{A}d\sigma_1\prod_{j=2}^{N}d^3r_j d\sigma_j=0, \quad l=i,f \tag{3.8}$$

where we have introduced the notation

$$\psi(\bar{1})=\psi(2,3,\ldots,N+1) . \tag{3.9}$$

The antisymmetrized wave function ψ_l^A can be written as

$$\psi_l^{A}=\frac{1}{\sqrt{N+1}}\sum_{j=1}^{N+1}(-1)^{j+1}\tilde{\psi}(\bar{j})v_l(j), \quad l=i,f \tag{3.10}$$

where

$$\tilde{\psi}(\bar{1})=[\psi_0(\bar{1})+\psi^{\text{pol}}(1;2,3,\ldots,N+1)] =[\psi_0(\bar{1})+\psi^{\text{pol}}(\bar{1})] . \tag{3.11}$$

If we use the notation

$$Y_{LS}^{*}(1)=Y_{L0}^{*}(\Omega_1)\chi_{1/2}(\sigma_1) ,$$

then the equation for v_L becomes

$$\int Y_{LS}^{*}(1)\psi_0^{*}(\bar{1})(H_1-k^2)\tilde{\psi}(\bar{1})v_L(1)d\sigma_1\prod_{i=2}^{N+1}d^3r_i d\sigma_i =N\int Y_{LS}^{*}(1)\psi_0^{*}(\bar{1})(H_1-k^2) \times\tilde{\psi}(\bar{2})v_L(2)d\sigma_1\prod_{i=2}^{N+1}d^3r_i d\sigma_i , \tag{3.12}$$

where the energy ϵ_1 in Eq. (3.6) has been replaced by k^2 for the continuum electron.

Now specializing to the problem of photoionization from neutral sodium atoms, we use the Hartree-Fock-Slater determinantal wave function for the unperturbed state ψ_0 of the atomic core. We write

$$\psi_0(\bar{1})=\frac{1}{\sqrt{10!}}\det|\,v_1(j),v_2(j),v_3(j),\ldots,v_{10}(j)\,|, \quad j\neq 1 \tag{3.13}$$

where

$$\left.\begin{matrix}v_1(1)\\ v_2(1)\end{matrix}\right\}=\frac{u_{1s}(r_1)}{r_1}Y_{00}(\Omega_1)\times\left\{\begin{matrix}\chi_{1/2}(\sigma_1)\\ \chi_{-1/2}(\sigma_1)\end{matrix}\right. ,$$

$$\left.\begin{matrix}v_3(1)\\ v_4(1)\end{matrix}\right\}=\frac{u_{2s}(r_1)}{r_1}Y_{00}(\Omega_1)\times\left\{\begin{matrix}\chi_{1/2}(\sigma_1)\\ \chi_{-1/2}(\sigma_1)\end{matrix}\right. ,$$

$$\left.\begin{matrix}v_5(1)\\ v_6(1)\end{matrix}\right\}=\frac{u_{2p}(r_1)}{r_1}Y_{10}(\Omega_1)\times\left\{\begin{matrix}\chi_{1/2}(\sigma_1)\\ \chi_{-1/2}(\sigma_1)\end{matrix}\right. ,$$

$$\left.\begin{matrix}v_7(1)\\ v_8(1)\end{matrix}\right\}=\frac{u_{2p}(r_1)}{r_1}Y_{11}(\Omega_1)\times\left\{\begin{matrix}\chi_{1/2}(\sigma_1)\\ \chi_{-1/2}(\sigma_1)\end{matrix}\right. ,$$

$$\left.\begin{matrix}v_9(1)\\ v_{10}(1)\end{matrix}\right\}=\frac{u_{2p}(r_1)}{r_1}Y_{1,-1}(\Omega_1)\times\left\{\begin{matrix}\chi_{1/2}(\sigma_1)\\ \chi_{-1/2}(\sigma_1)\end{matrix}\right. .$$

The radial orbitals u_{nl} are the Hartree-Fock (HF) orbitals and they have been calculated by Clementi and Roetti.[7]

The polarized part of the wave function, which is the essence of POM,[1] is derived from the unperturbed ground atomic core state ψ_0 by assuming it to be adiabatically perturbed by the outer electron. In the adiabatic approximation, only the dipole part of the interaction between the outer electron and the core is included and it is assumed that the outer electron remains stationary while the target electrons are being perturbed. This perturbation is then

$$V_{\rm ad}=\sum_{j=2}^{11}\frac{2}{r_{1j}}-\frac{2(Z-1)}{r_1}$$
$$\cong\frac{2}{r_1^2}\sum_{j=2}^{11}r_j\cos\theta_{1j}\epsilon(r_1,r_j)\ . \qquad (3.14)$$

We notice that by introducing the step function[8] $\epsilon(r_1,r_j)$, the polarization effect is included only when the outer electron is outside the atomic orbitals. Similar to Eq. (3.13), the polarized core can be written as

$$\tilde{\psi}(\bar{1})=\psi_0(\bar{1})+\psi^{\rm pol}(\bar{1})$$
$$=\frac{1}{\sqrt{10!}}\det|\phi_1(j),\phi_2(j),\ldots,\phi_{10}(j)|,\quad j\neq 1 \qquad (3.15)$$

where

$$\phi_i(j)=v_i(j)+\frac{v_i'(j)}{r_1^2}\ . \qquad (3.16)$$

The perturbed orbitals v_i' in Eq. (3.16) can be expressed as

$$v_i'(j)=\sum_{l',m'}C_{nl\to l'}^{m\to m'}\frac{u_{nl\to l'}(r_j)}{r_j}$$
$$\times Y_{1,-\mu}(\Omega_1)Y_{l'm'}^*(\Omega_j)\epsilon(r_1,r_j)$$
$$\times\begin{cases}x_{1/2}(\sigma_1), & i\ \text{odd}\\ x_{-1/2}(\sigma_1), & i\ \text{even}\end{cases} \qquad (3.17)$$

where $i,j=2,3,\ldots,11$ and where

$$C_{nl\to l'}^{m\to m'}=(-1)^{\mu}\frac{8\pi}{3}\left[\frac{3}{4\pi}\frac{2l+1}{2l'+1}\right]^{1/2}C_{000}^{l1l'}C_{m\mu m'}^{l1l'}\ , \qquad (3.18)$$

the C's being the Clebsch-Gordan coefficients. The radial parts of the perturbed orbitals $u_{nl\to l'}(r)$ are obtained from the equation[9]

$$\left[\frac{d^2}{dr^2}-\frac{1}{u_{nl}(r)}\left[\frac{d^2}{dr^2}u_{nl}(r)\right]+\frac{l(l+1)-l'(l'+1)}{r^2}\right]u_{nl\to l'}(r)=ru_{nl}(r)\ . \qquad (3.19)$$

The Sternheimer approximation may not be accurate because exchange is not correctly taken into account.[1] In the numerical solutions, the singularities in the second term due to nodes in the target functions have to be smoothed out. If an accurate version of perturbation theory is used then exchange would be included, as was done by Bhatia *et al.*,[10] and these singularities would not arise. We have calculated all the polarized orbitals $(1s\to p)$, $(2s\to p)$, $(2p\to s)$, and $(2p\to d)$ using Eq. (3.19).

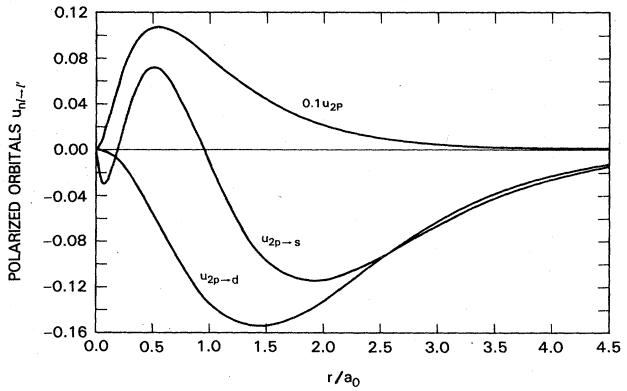

FIG. 1. Polarized orbitals $(2p\to d)$ and $(2p\to s)$ obtained using Sternheimer's approximation, and the unperturbed orbital u_{2p}.

These orbitals are made orthogonal to all bound orbitals of the same symmetry. Because of the $1s$ orbitals being tightly bound, the contribution from $(1s\to p)$ orbitals to the polarizability of the Na^+ ion is very small. Therefore, we have neglected its contribution in the exchange polarization terms (although, we have added the contribution due to this perturbed orbital in the direct polarization potential). Figure 1 shows the perturbed orbitals $u_{2p\to s}$ and $u_{2p\to d}$ and the unperturbed orbital u_{2p} of the sodium ion as a function of position r. As expected, the perturbed orbitals are much smaller in magnitude compared to the unperturbed orbital. Figure 2 shows the perturbed orbitals $u_{2s\to p}$ and the unperturbed orbital u_{2s}. The unperturbed orbital u_{1s} is not shown in Fig. 2 as it peaks around $r=0.1$ and falls off very rapidly. Again, the perturbed orbitals, in particular $u_{1s\to p}$, are very small in comparison to the unperturbed orbitals.

Thus, after constructing the unperturbed ground ionic core ψ_0 and the perturbed core $(\psi_0+\psi^{\rm pol})$ from the bound and perturbed atomic orbitals we can explicitly derive the equation satisfied by the outer electron from Eq. (3.12). The resulting integro-differential equation satisfied by the outer electron is

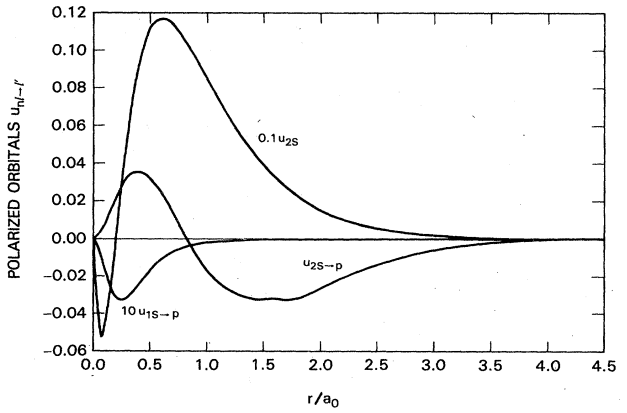

FIG. 2. Polarized orbitals $(2s\to p)$ and $(1s\to p)$ obtained using Sternheimer's approximation and the unperturbed orbital u_{2s}.

$$\left[\frac{d^2}{dr^2}-\frac{L(L+1)}{r^2}+k^2\right]u_{kL}(r) =[V_C(r)+V_p(r)+W]u_{kL}(r)\ , \quad (3.20)$$

where

$$u_L(\vec{r})=\frac{u_{kL}(r)}{r}Y_{L0}(\Omega)x_{1/2}(\sigma)\ .$$

In Eq. (3.20), V_C is the direct static potential, V_p is the direct polarization potential. The expressions for these potentials are as follows:

$$V_C(r)=4\Gamma^0(1s,1s;r)+4\Gamma^0(2s\,2s;r) +12\Gamma^0(2p,2p;r)-\frac{2Z}{r}\ , \quad (3.21)$$

$$V_p(r)=-[I_{1s\to p}(r)+I_{2s\to p}(r)+I_{2p\to d}(r)]\ , \quad (3.22)$$

where

$$I_{nl\to l'}(r)=\frac{1}{r^4}\frac{8}{3}\left[\int_0^r u_{nl}(x)u_{nl\to l'}(x)x\,dx-\sum_{n,l'}\int_0^r u_{nl\to l'}(x)u_{nl'}(x)dx\int_0^r u_{nl'}(x)u_{nl}(x)x\,dx\right], \quad (3.23)$$

except

$$I_{2p\to d}(r)=\frac{16}{3}\frac{1}{r^4}\int_0^r u_{2p}(x)xu_{2p\to d}(x)dx \quad (3.24)$$

and

$$Wu_{kL}(r)=[W_{ex}u_{kL}(r)+W_{ep}u_{kL}(r)]\ . \quad (3.25)$$

In Eq. (3.25) $W_{ex}u_{kL}(r)$ and $W_{ep}u_{kL}(r)$ are exchange and exchange-polarization terms, respectively, and they are as follows:

$$W_{ex}u_{kL}(r)=-\frac{2}{2L+1}u_{1s}(r)\Gamma^L(1s,kL;r)-\frac{2}{2L+1}u_{2s}(r)\Gamma^L(2s,kL;r)-3\sum C_{1L\lambda}\Gamma^\lambda(2p,kL;r)u_{2p}(r) +\delta_{lL}(k^2+\epsilon_{nl})u_{nl}(r)\int_0^\infty u_{kL}(r')u_{nl'}(r')dr'\ , \quad (3.26)$$

$$W_{ep}u_{kL}(r)=-r\{W^0_{ep}(r)+\delta_{L0}[2I^0_{ep}(r)+2J^{2p,2p\to s}(r)]+\delta_{L1}[2I^1_{ep}(r)+\tfrac{2}{3}J^{2s,2s\to p}(r)]+\delta_{L2}[2I^2_{ep}(r)+\tfrac{4}{5}J^{2p,2p\to d}(r)]\}\ , \quad (3.27)$$

where

$$J^{nl,nl\to l'}(r)=-\frac{1}{r}\left\{\left[\frac{d^2}{dr^2}+\frac{2Z}{r}-\frac{l'(l'+1)}{r^2}+k^2\right]u_{nl\to l'}(r)\int_r^\infty\frac{u_{nl}(r_1)u_{kL}(r_1)}{r_1^2}dr_1 +\left[-\frac{2}{r^2}u_{nl}(r)\frac{d}{dr}u_{nl\to l'}(r)-\left[\frac{1}{r^2}\frac{d}{dr}u_{nl}(r)-\frac{2}{r^3}u_{nl}(r)\right]u_{nl\to l'}(r)\right]u_{kL}(r) -\frac{1}{r^2}u_{nl}(r)u_{nl\to l'}(r)\frac{du_{kL}(r)}{dr}\right\}, \quad (3.28)$$

and

$$W^0_{ep}(r)=\frac{4}{2L+1}\left[\delta_{\lambda,L+1}\frac{L+1}{2L+3}+\delta_{\lambda,L-1}\frac{L}{2L-1}\right]\frac{u_{2s\to p}(r)}{r}r^\lambda\int_r^\infty\frac{u_{2s}(r_1)u_{kL}(r_1)}{r_1^{\lambda+3}}dr_1 +\frac{4}{2L+1}\delta_{\lambda L}\frac{u_{2p\to s}(r)}{r}r^\lambda\int_r^\infty\frac{u_{2p}(r_1)}{r_1^{\lambda+3}}u_{kL}(r_1)dr_1 +\sum_\lambda 8\begin{bmatrix}\lambda & L & 2\\ 0 & 0 & 0\end{bmatrix}^2\frac{u_{2p\to d}(r)}{r}r^\lambda\int_r^\infty\frac{u_{2p}(r_1)u_{kL}(r_1)}{r_1^{\lambda+3}}dr_1\ . \quad (3.29)$$

The explicit forms of the exchange polarization terms $I^0_{ep}(r)$, $I^1_{ep}(r)$, and $I^{(2)}_{ep}(r)$ are given in Appendix A. In these equations,

$$\Gamma^{\lambda}(nl,n'l';r)=\int_0^{\infty} u_{nl}(x)u_{n'l'}(x)g_{\lambda}(x,r)dx \ , \qquad (3.30)$$

where

$$g_{\lambda}(x,y)=\begin{cases} x^{\lambda}/y^{\lambda+1}, & x<y \\ y^{\lambda}/x^{\lambda+1}, & x>y \ . \end{cases} \qquad (3.31)$$

The indices $n'l'$ in Eq. (3.30) refer to bound as well as continuum electron kl', and ϵ_{nl} are the orbital energies. The direct polarization potential $V_p(r)$ given by Eq. (3.22) is shown in Fig. 3. We see that close to the origin it has a very attractive part followed by a repulsive part. However, it behaves properly in the asymptotic region, that is

$$V_p(r)\rightarrow -\frac{\alpha}{r^4} \quad \text{as } r\rightarrow\infty \ ,$$

where α is the electrostatic dipole polarizability of Na^+. The polarizability obtained in this calculation is $1.0914a_0^3$, compared to the value of $\alpha=0.9459a_0^3$ as obtained by Lahiri and Mukherji.[11] The individual contributions are $\alpha_{1s\rightarrow p}=0.0005a_0^3$, $\alpha_{2s\rightarrow p}=0.0337a_0^3$, $\alpha_{2p\rightarrow s}=0.1690\alpha_0^3$, and $\alpha_{2p\rightarrow d}=0.8882a_0^3$. However, a more recent calculation[12] based on quantum defect obtained by using very accurately measured energy levels gives $\alpha=1.0015a_0^3$. As mentioned before, both the bound-state wave function for the $3s$ valence electron and the continuum-state wave function for the photoejected electron are calculated using Eq. (3.20). The equation is solved in both cases in (i) the exchange approximation, (ii) the exchange-adiabatic approximation, and (iii) the polarized-orbital (PO) approximation. The latter corresponds to keeping all the terms in the equation. Neglecting $V_p(r)$ and $W_{ep}(r)$ in Eq. (3.20) corresponds to the exchange approximation and neglecting only $W_{ep}(r)$ we get the equation in the exchange-adiabatic approximation. It should be mentioned that the orthogonality terms appearing in Eq. (3.26)

$$\delta_{lL}(k^2+\epsilon_{nl})u_{kL}(r)\int_0^{\infty} u_{kL}(r)u_{nl}(r)dr$$

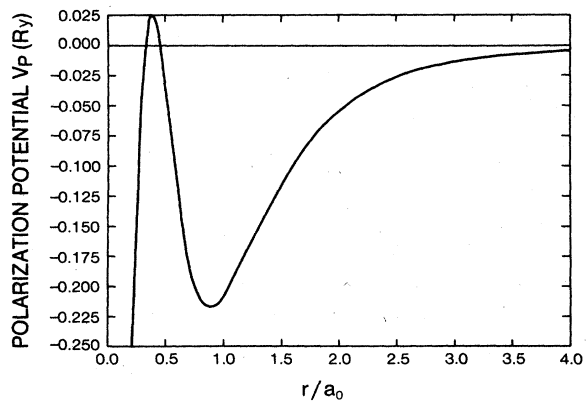

FIG. 3. Polarization potential V_p using the polarized orbitals.

are set equal to zero in solving Eq. (3.20) in all three approximations. It has been shown by LaBahn[13] that if the polarization potential $V_p(r)$ is chosen consistently, as was done here by the HF perturbation theory, the orthogonality constraint has little effect on the scattering functions and therefore, on phase shifts. The integro-differential equation given by Eq. (3.20) was solved by using a "modified Nordsieck" predictor-corrector method.[14]

In calculating the bound-state wave functions Eq. (3.20) is solved for $l=0$, letting the energy k^2 go into an eigenvalue

$$k^2\rightarrow -I_{3s} \ ,$$

where I_{3s} is the binding energy of the $3s$ electron in the appropriate approximation. A comparison of the binding energies in various approximations is given in Table I. They are also compared to other calculated values[7,15] and to the experimental ionization energy[16] of the sodium atom. We see clearly from the table that including polarization and exchange polarization (full POM) gives the closest agreement with the experiment.[16] Table II lists the bound-state functions in the three different approximations.

The integro-differential Eq. (3.20) was solved for the p-wave continuum function for the photoelectron for several k values, starting from threshold, in the three approximations. The asymptotic form of the radial wave function in a modified Coulomb field is given by the well-known expression

$$u_{kl}(r)\rightarrow \frac{1}{k}\sin\left[kr-\frac{l\pi}{2}-\gamma\ln(2kr)+\sigma_l+\delta_l\right], \quad \text{as } r\rightarrow\infty \qquad (3.32)$$

where

$$\gamma=-\frac{1}{k}$$

and $\sigma_l=\arg\Gamma(l+1+i\gamma)$ is the Coulomb phase shift. The phase shift δ_l in Eq. (3.32) is the additional phase shift due to the departure from pure Coulomb scattering at small distances. Thus Eq. (3.32) was used to extract the phase shifts for s, p, and d waves in all the approximations. We note here that, as mentioned earlier, for pho-

TABLE I. Binding energy of the $3s$ orbital of the sodium ground state in various approximations.

Approximation	Binding energy (Ry)
Exchange	0.3636
Exchange adiabatic	0.3774
Polarized orbital	0.3780
Many-body perturbation[a]	0.3792
Hartree-Fock[b]	0.3642
Experiment[c]	0.3778

[a]Reference 15.
[b]Reference 7.
[c]Reference 16.

TABLE II. Bound-state wave functions for the valence $3s$ orbital in various approximations.

r/a_0	Exchange approx.	Exchange-adiabatic approx.	Polarized-orbital approx.
0.0	0.0	0.0	0.0
0.05	0.071 35	0.075 70	0.084 05
0.15	0.038 28	0.040 21	0.050 91
0.2	−0.005 17	0.006 08	−0.008 24
0.3	−0.086 06	−0.091 99	−0.114 81
0.5	−0.156 76	−0.1666	−0.179 24
0.7	−0.1297	−0.137 23	−0.135 28
0.9	−0.057 63	−0.059 47	−0.056 94
1.0	−0.015 11	−0.013 62	−0.012 74
1.05	0.006 72	0.009 87	0.009 94
1.15	0.050 55	0.056 97	0.055 64
1.35	0.1355	0.147 75	0.145 22
1.5	0.194 68	0.210 30	0.208 02
1.7	0.265 57	0.284 35	0.283 28
2.15	0.389 13	0.409 83	0.411 56
2.6	0.4656	0.483 25	0.486 37
3.0	0.500 33	0.513 16	0.516 68
3.3	0.509 84	0.518 61	0.522 18
3.6	0.508 12	0.512 82	0.507 17
4.8	0.432 32	0.424 43	0.419 32
6.3	0.290 47	0.276 92	0.273 28
8.1	0.154 55	0.142 83	0.140 79
9.9	0.074 52	0.069 35	0.065 91
15.0	0.007 09	0.005 92	0.005 81
20.0	0.000 57	0.000 44	0.000 43

toionization calculations we need to solve the scattering equation only for $l=1$ for the continuum function. The s-, p-, and d-wave phase shifts at various electron energies are listed in Tables III, IV, and V. The right-hand columns of Tables III, IV, and V contain the phase shifts derived from the experimentally measured quantum defects.[17] We notice that our calculated phase shifts in the exchange-adiabatic approximation are in better agreement with the quantum-defect results than the PO results. The close agreement of these phase shifts, when calculated including polarization, with the accurately measured quantum-defect results is very encouraging.

These phase shifts were used to calculate the "reduced" differential cross section for electron scattering from the Na^+ ion. The reduced differential cross section $R(\theta)$ is given by

$$R(\theta)=\frac{I(\theta)}{I_C(\theta)}\ , \tag{3.33}$$

where $I_C(\theta)$ is the differential cross section due to a pure Coulomb field,

$$I_C(\theta)=\left[\frac{1}{2k^2\sin^2(\theta/2)}\right]^2\ , \tag{3.34}$$

and

$$I(\theta)=|f(\theta)|^2$$

with

$$f(\theta)=\frac{1}{2ik}\sum_{l=0}^{\infty}(2l+1)P_l(\cos\theta)(e^{2i(\sigma_l+\delta_l)}-1)\ . \tag{3.35}$$

Equation (3.34) is the Rutherford formula for scattering through an angle θ. It can be shown that

$$R(\theta)=X^2+Y^2\ ,$$

where

$$\begin{aligned} X&=1-\frac{2\sin^2(\theta/2)}{r}\sum_l(2l+1)P_l(\cos\theta)\cos p_l\sin\delta_l\ ,\\ Y&=-\frac{2\sin^2(\theta/2)}{r}\sum_l(2l+1)P_l(\cos\theta)\sin p_l\sin\delta_l\ , \end{aligned} \tag{3.36}$$

TABLE III. s-wave phase shifts in rad (relative to pure Coulomb phase shift) for $e+Na^+$ scattering.

k (a.u.)	Exchange approx. δ_0 (rad)	Exchange-adiabatic approx. δ_0 (rad)	Polarized-orbital approx. δ_0 (rad)	Quantum defect[a] δ_0 (rad)
0.1	4.151	4.227		4.2328
0.2	4.146	4.221		4.2271
0.3	4.137	4.212	4.205	4.2178
0.4	4.126	4.198	4.192	4.2053
0.5	4.111	4.181	4.177	4.1901
0.6	4.093	4.161	4.158	
0.7	4.071	4.138	4.136	
0.8	4.047	4.112	4.111	
0.9	4.020	4.083	4.083	
1.0	3.991	4.052	4.053	
1.1	3.960	4.019	4.020	
1.2	3.927	3.984	3.985	
1.3	3.892	3.948	3.950	
1.4	3.857	3.911	3.913	
1.5	3.820	3.874	3.875	

[a]Reference 17.

TABLE IV. p-wave phase shifts in rad (relative to pure Coulomb phase shift) for $e + Na^+$ scattering.

k (a.u.)	Exchange approx. δ_1 (rad)	Exchange-adiabatic approx. δ_1 (rad)	Polarized-orbital approx. δ_1 (rad)	Quantum defect[a] δ_1 (rad)
0.1	2.624	2.687	2.691	2.6814
0.2	2.613	2.676	2.680	2.6712
0.3	2.597	2.659	2.666	2.6549
0.4	2.575	2.637	2.643	2.6336
0.5	2.548	2.609	2.615	2.6085
0.6	2.517	2.577	2.583	
0.7	2.483	2.543	2.548	
0.8	2.447	2.506	2.511	
0.9	2.410	2.468	2.473	
1.0	2.372	2.430	2.434	
1.1	2.334	2.391	2.395	
1.2	2.296	2.352	2.357	
1.3	2.259	2.314	2.319	
1.4	2.223	2.277	2.281	
1.5	2.188	2.241	2.245	

[a]Reference 17.

and

$$p_l(\theta,r)=2(\sigma_l-\sigma_0)+2\gamma\ln[\sin(\theta/2)]+\delta_l\ .$$

The phase shifts calculated for s, p, and d waves are used to calculate the reduced differential cross sections. These are listed in Table VI. These cross sections agree very well with those obtained by Seaton[18] using the quantum-defect method.

IV. PHOTOIONIZATION CROSS SECTIONS

Now that we have the bound-state wave function for the valence $3s$ electron for the sodium atom and the continuum wave function for the photoejected electron we have the total wave function for the system ψ_i in the initial state and ψ_f in the final state. Thus, using Eq. (2.1) we now calculate the photoionization cross sections.

In the formula given by Eq. (2.1), $4\pi\alpha a_0^2=2.568\times10^{-18}$ cm^2. We notice that the formula for the cross section is given in the length form. In the polarized-orbital method, the basis assumption is that the core is polarized only when the outer electron (valence or continuum) is outside the core electron. Hence the transition operator which emphasizes the asymptotic region of the wave functions should be used in this application and thus it is the length form of the matrix element which is most appropriate for this method.

The matrix element M given by

TABLE V. d-wave phase shifts in rad (relative to pure Coulomb phase shift) for $e + Na^+$ scattering.

k (a.u.)	Exchange approx. δ_2 (rad)	Exchange-adiabatic approx. δ_2 (rad)	Polarized-orbital approx. δ_2 (rad)	Quantum defect[a] δ_2 (rad)
0.1	0.019	0.051	0.059	0.0481
0.2	0.021	0.054	0.057	0.0521
0.3	0.026	0.062	0.065	0.0589
0.4	0.032	0.072	0.074	0.0685
0.5	0.040	0.084	0.084	0.0811
0.6	0.051	0.099	0.096	
0.7	0.063	0.117	0.110	
0.8	0.079	0.137	0.125	
0.9	0.096	0.159	0.142	
1.0	0.116	0.183	0.161	
1.1	0.138	0.209	0.182	
1.2	0.161	0.235	0.205	
1.3	0.186	0.263	0.228	
1.4	0.211	0.290	0.253	
1.5	0.238	0.318	0.278	

[a]Reference 17.

TABLE VI. Reduced differential cross sections $R(\theta)$ in polarized-orbital approximation for $e + Na^+$ scattering.

θ (deg)	$R(\theta)$ $k=0.3$ a.u.	$k=0.4$ a.u.	$k=0.5$ a.u.	$k=0.6$ a.u.
0	1.0	1.0	1.0	1.0
10	0.993	1.029	0.987	0.965
20	1.072	0.903	1.011	1.143
30	0.855	1.092	1.282	1.213
40	1.040	1.361	1.189	0.896
50	1.366	1.179	0.777	0.476
60	1.250	0.764	0.419	0.265
70	0.899	0.483	0.331	0.358
80	0.659	0.451	0.478	0.645
90	0.602	0.559	0.689	0.921
100	0.611	0.646	0.797	1.016
110	0.579	0.620	0.727	0.870
120	0.490	0.491	0.517	0.553
130	0.389	0.329	0.270	0.221
140	0.332	0.214	0.096	0.023
150	0.340	0.181	0.048	0.029
160	0.395	0.218	0.105	0.191
170	0.455	0.276	0.193	0.380
180	0.481	0.302	0.233	0.461

$$M=\left\langle \psi_f \left| \sum_{i=1}^{11} z_j \right| \psi_i \right\rangle \tag{4.1}$$

can be written as a sum of zeroth-, first-, and second-order terms, M_1, M_2, and M_3, respectively. Thus

$$M=M_1+M_2+M_3 ,$$

where

$$M_1=\frac{1}{11}\left\langle A\{v_L(1)\psi_0(\bar{1})\} \left| \sum_{j=1}^{11} z_j \right| A\{v_b(1)\psi_0(\bar{1})\} \right\rangle , \tag{4.2}$$

$$M_2=\frac{1}{11}\left\langle A\{v_L(1)\psi^{\rm pol}(\bar{1})\} \left| \sum_{j=1}^{11} z_j \right| A\{v_b(1)\psi_0(\bar{1})\} \right\rangle + \frac{1}{11}\left\langle A\{v_L(1)\psi_0(\bar{1})\} \left| \sum_{j=1}^{11} z_j \right| A\{v_b(1)\psi^{\rm pol}(\bar{1})\} \right\rangle , \tag{4.3}$$

and

$$M_3=\frac{1}{11}\left\langle A\{v_L(1)\psi^{\rm pol}(\bar{1})\} \left| \sum_{j=1}^{11} z_j \right| A\{v_b(1)\psi^{\rm pol}(\bar{1})\} \right\rangle . \tag{4.4}$$

The reason for dividing M into components is that previous calculations[3] on photoionization of the sodium atom have been performed including M_1 and M_2 only. In the exchange and exchange-adiabatic approximations M_2 and M_3 are neglected, and in the PO approximation all three of them are included in the matrix element M. The significance of the contribution of M_3, that is, the polarization terms in the photoionization matrix element, has been assessed and found to be important when compared to the accurate many-body theoretical results[19] in Li photoionization.[2] The explicit forms of the matrix elements M_1, M_2, and M_3 are given in Appendix B. In Table VII, we give the numerical values of the photoionization cross sections as a function of the photoelectron energy k^2 along with other results. This calculation was carried out up to a photon energy of 60 eV. Beyond that energy, photoionization cross sections were not calculated since the POM is expected to be good only for low energies, in fact, 60 eV may already be too high. Figure 4 shows the cross sec-

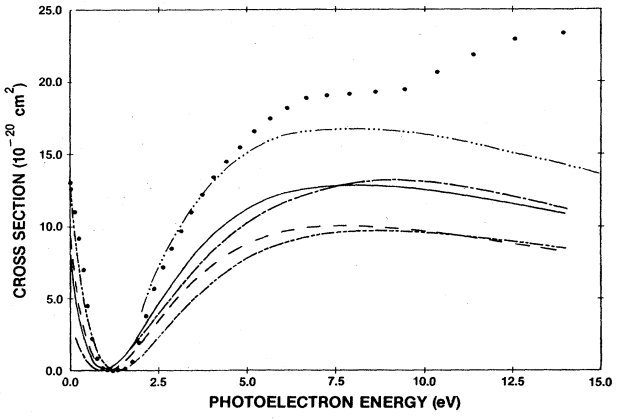

FIG. 4. Photoionization cross section of the sodium atom vs the energy of the ejected electron. ——, PO approximation; ----, exchange-adiabatic approximation; — — —, exchange approximation; —·—·—, results obtained by Chang and Kelly; — · · · —, cross sections obtained by Chang. Experimental results of Hudson and Carter are shown as points on the graph.

TABLE VII. Photoionization cross sections of the Na atom in several different approximations (in units of 10^{-20} cm^2).

k (a.u.)	Photon energy (eV)	Exchange approx.	Exchange-adiab. approx.	Pol.-orb. approx.	σ^a	σ^b	σ^c
0.0	5.1425	9.297	12.808	8.419			8.496
0.1	5.2786	6.417	9.355	5.748	6.612	2.309	5.390
0.2	5.6867	1.546	3.049	1.228	1.632	0.413	1.142
0.3	6.3670	0.0738	0.031	0.319	0.058	0.363	0.264
0.4	7.3194	2.446	1.435	3.536	2.375	2.972	3.513
0.5	8.544	6.003	4.749	7.832	5.933	6.655	7.773
0.6	9.6406	8.674	7.643	11.111	8.622	10.051	11.416
0.7	11.8094	9.894	9.259	12.627	9.875	12.133	13.411
0.8	13.8502	9.949	9.692	12.815	9.959	13.119	13.740
0.9	16.1632	9.315	9.346	12.157	9.339	12.709	12.957
1.0	18.7483	8.374	8.597	11.047	8.411	11.413	12.102
1.1	21.6055	7.357	7.698	9.934	7.395	9.931	10.892
1.2	24.7349	6.391	6.792	8.602	6.435	9.148	
1.3	28.1363	5.527	5.951	7.714			
1.4	31.8099	4.478	5.206	6.893			
1.5	35.7556	4.146	4.556	6.134			
1.6	39.9734	3.610	3.999	5.361			
1.7	44.4633	3.159	3.524	4.843			
1.8	49.2254	2.780	3.117	4.392			
1.9	54.2595	2.459	2.769	3.905			
2.0	59.5658	2.185	2.470	3.507			

[a]Lowest-order contribution in the nonrelativistic calculation [using the length form of Chang and Kelly (Ref. 5)].

[b]Final nonrelativistic calculation including correlation effects (in velocity form) in Chang and Kelly (Ref. 5).

[c]Close-coupling results (interpolated) in Butler and Mendoza (Ref. 20).

tions as a function of photoelectron energy. Other theoretical cross sections and the experimental results[4] are also shown in the graph. The calculated values of the cross section at the spectral head ($k^2=0$) are quite different in the three approximations as can be seen from Table VII and Fig. 4. Almost complete cancellation of the positive and negative portions of the integrands in the photoionization matrix element accounts for this. However, our result at the spectral head in the PO approximation is close to that obtained by Butler and Mendoza (Ref. 20) who carried out a close-coupling calculation. Our low-energy results in the PO approximation are very close to those given in Ref. 20. The first calculation for photoionization of the sodium atom was worked out by Seaton[21] using the HF wave functions. Our results in the exchange approximation agree very well with Seaton's results, as expected. Both of these in turn are essentially those obtained by Chang and Kelly[5] in their lowest-order approximation. None of these theoretical results, however, agree well with the experimental[4] ones. The agreement with the experiment for the photoionization cross section in the exchange-adiabatic approximation is quite good from threshold to about 2 eV of photoelectron energy above the threshold. Beyond that they differ considerably, the experimental results being always much higher than the theoretical results.

The inclusion of the exchange polarization terms both in obtaining the wave functions as well as in the photoionization matrix element, to improve accuracy, leads to the PO approximation, the central topic of this research. We notice from Fig. 4 that, after the minimum, the cross sections obtained in the PO approximation are always higher than those obtained in the exchange and in the exchange-adiabatic approximations. Thus even though our results in the PO approximation are closer to the experimental values up to about 10 eV of photoelectron energy, they are far from being close beyond that energy. From 10 to 54 eV of photoelectron energy all theoretical curves decrease, while the experimental curve increases. In Fig. 4 we have also included the results of the many-body perturbation calculations of Chang and Kelly.[5] Beyond the minimum, Chang[15] has also carried out a many-body perturbation calculation in which the effects of virtual excitations of the inner-shell electrons have been included by calculating the lowest diagrammatic terms using orbitals obtained from a long-range polarization potential instead of evaluating an infinite sum of diagrams corresponding to virtual excitations of Hartree-Fock orbitals. However, the cross sections obtained are sensitive[22] to the choice of the long-range polarization potential. The results of Chang obtained by using a length approximation for a cross section are also shown in Fig. 4 and they are seen to be higher than the other calculated cross sections shown, but closer to the experimental results.

As indicated above, the results at low energies in the PO approximation are less than the exchange-adiabatic

and experimental results. An attempt was made to improve these results in the PO approximation by retaining only the $(2p\rightarrow d)$ orbital in Eq. (3.20). This orbital was modified to give the experimental binding energy 0.3778 Ry when solving for the bound-state function from Eq. (3.20). The modified orbital gives $\alpha=0.995a_0^3$ and the photoionization cross sections below the minimum improve considerably, being close to the full exchange-adiabatic but still below the experimental results. The cross sections beyond the minimum are substantially smaller than the full exchange-adiabatic and PO results. However, since there are still questions about the accuracy of the experimental results (cf. the Conclusion) we believe the $(2p\rightarrow d)$ polarized-orbital results may still have merit.

V. CONCLUSION

The agreement of our results in the polarized-orbital approximation with the extensive calculations of Chang and Kelly[5] give us much reason to believe in the applicability of the POM for photoionization of sodium and other alkali-metal atoms. Even though our results differ from the experimental results beyond a few electron volts of photoelectron energy, our results, like other theoretical calculations, do not reveal the hump seen in the experimental curve. As pointed out by Chang,[15] since the molecular photoabsorption cross section is almost 2 orders of magnitude larger than the atomic photoabsorption cross section, even the presence of small amounts of molecular vapor could increase the observed photoionization cross section to a significant extent. Thus we believe this may be the source of the experimental enhancement in this as well as other alkali-metal photoionization cross sections.

A recent close-coupling calculation by Butler and Mendoza[20] does not give the hump in the photoionization cross section. They also find that the experimental results are too high and renormalization of the experimental results by multiplying by 0.7 gives good agreement with the calculated values. Though the results of Chang[15] agree with the experimental results as they exist, the closeness of the present calculations and those of Refs. 5 and 20 is significant. Thus we believe further experimental investigation is desirable.

ACKNOWLEDGMENTS

We wish to thank Dr. A. Temkin for suggesting this investigation. We thank Dr. R. J. Drachman and Dr. Temkin for numerous helpful discussions during the course of this work. We also wish to thank Mr. E. C. Sullivan for his advice and help in the computational part of this work. We thank Dr. K. Butler for sending his numerical results. One of us (A.D.) gratefully acknowledges support by the National Aeronautics and Space Administration. This work is based on the thesis submitted by A.D. to the University of Maryland in partial fulfillment of the requirements for the Ph.D. degree. A.D. gratefully acknowledges the generous help by Professor J. Sucher during all phases of the research.

APPENDIX A

The explicit forms of the integrals $I^0_{\rm ep}(r)$, $I^1_{\rm ep}(r)$, and $I^2_{\rm ep}(r)$ appearing in Eq. (3.27) are as follows:

$$
\begin{aligned}
I^0_{\rm ep}(r)=&-\frac{4}{5}\frac{u_{2p\rightarrow d}(r)}{r}\left[\int_r^\infty \frac{u_{kL}(r_1)u_{2p}(r_1)}{r_1^2}dr_1\right]\Gamma^2(2p,2p;r)\\
&-\frac{u_{2p\rightarrow s}(r)}{r}\left[\int_r^\infty \frac{u_{kL}(r_1)u_{2p}(r_1)}{r_1^2}dr_1\right][4\Gamma^0(1s,1s;r)+4\Gamma^0(2s,2s;r)+10\Gamma^0(2p,2p;r)]\\
&-\frac{2}{3}\frac{u_{2s\rightarrow p}(r)}{r}\left[\int_r^\infty \frac{u_{kL}(r_1)u_{2p}(r_1)}{r_1^2}dr_1\right]\Gamma^1(2s,2s;r)\\
&+\frac{u_{2p}(r)}{r}\left[\int_0^\infty \frac{u_{kL}(r_1)u_{2p}(r_1)}{r_1^2}dr_1\right.\\
&\quad\times\left[\tfrac{8}{3}\int_0^{r_1} u_{2p\rightarrow d}(r_2)u_{2p}(r_2)g_1(r,r_2)dr_2-\tfrac{2}{3}\int_0^{r_1} u_{2p\rightarrow s}(r_2)u_{2p}(r_2)g_1(r,r_2)dr_2\right.\\
&\quad\left.\left.+\tfrac{4}{3}\int_0^\infty u_{2s\rightarrow p}(r_2)u_{2s}(r_2)g_1(r,r_2)dr_2\right]\right]\\
&-2\frac{u_{1s}(r)}{r}\left[\int_0^\infty \frac{u_{kL}(r_1)u_{2p}(r_1)}{r_1^2}dr_1\int_0^{r_1} u_{1s}(r_2)u_{2p\rightarrow s}(r_2)g_0(r,r_2)dr_2\right]\\
&-\frac{2u_{2s}(r)}{r}\left[\int_0^\infty \frac{u_{kL}(r_1)u_{2p}(r_1)}{r_1^2}dr_2\int_0^{r_1} u_{2s}(r_2)u_{2p\rightarrow s}(r_2)g_0(r,r_2)dr_2\right],
\end{aligned}
$$

$$
\begin{aligned}
I^1_{\mathrm{ep}}(r) = &-\frac{4}{9}\frac{u_{2p\to d}(r)}{r}\left[\int_r^\infty \frac{u_{kL}(r_1)u_{1s}(r_1)}{r_1^2}dr_1\right]\Gamma^1(2p,1s;r)\\
&-\frac{4}{9}\frac{u_{2p\to d}(r)}{r}\left[\int_r^\infty \frac{u_{kL}(r_1)u_{2s}(r_1)}{r_1^2}dr_1\right]\Gamma^1(2p,2s;r)\\
&+\frac{8}{9}\frac{u_{1s}(r)}{r}\left[\int_0^\infty \frac{u_{kL}(r_1)u_{1s}(r_1)}{r_1^2}dr_1\int_0^{r_1} u_{2p\to d}(r_2)u_{2p}(r_2)g_1(r,r_2)dr_2\right]\\
&+\frac{8}{9}\frac{u_{2s}(r)}{r}\left[\int_0^\infty \frac{u_{kL}(r_1)u_{2s}(r_1)}{r_1^2}dr_1\int_0^{r_1} u_{2p\to d}(r_2)u_{2p}(r_2)g_1(r,r_2)dr_2\right]\\
&+\frac{2}{3}\frac{u_{2s\to p}(r)}{r}\left[\int_r^\infty \frac{u_{kL}(r_1)u_{2s}(r_1)}{r_1^2}dr_1\right][2\Gamma^0(1s,1s;r)+\Gamma^0(2s,2s;r)+6\Gamma^0(2p,2p;r)]\\
&-\frac{2}{3}\frac{u_{2s\to p}(r)}{r}\left[\int_r^\infty \frac{u_{kL}(r_1)u_{1s}(r_1)}{r_1^2}dr_1\right]\Gamma^0(1s,1s;r)\\
&-\frac{2}{9}\frac{u_{2p\to s}(r)}{r}\left[\int_r^\infty \frac{u_{kL}(r_1)u_{1s}(r_1)}{r_1^2}dr_1\right]\Gamma^1(1s,2p;r)\\
&-\frac{2}{9}\frac{u_{2p\to s}(r)}{r}\left[\int_r^\infty \frac{u_{kL}(r_1)u_{2s}(r_1)}{r_1^2}dr_1\right]\Gamma^1(2s,2p;r)\\
&+\frac{2}{9}\frac{u_{2s}(r)}{r}\left[\int_0^\infty \frac{u_{kL}(r_1)u_{2s}(r_1)}{r_1^2}dr_1\left[\int_0^{r_1} u_{2s\to p}(r_2)u_{2s}(r_2)g_1(r,r_2)dr_2\right.\right.\\
&\qquad\left.\left.+2\int_0^{r_1} u_{2p\to s}(r_2)u_{2p}(r_2)g_1(r,r_2)dr_2\right]\right]\\
&+\frac{4}{9}\frac{u_{1s}(r)}{r}\left[\int_0^\infty \frac{u_{kL}(r_1)u_{1s}(r_1)}{r_1^2}dr_1\left[\int_0^{r_1} u_{2s\to p}(r_2)u_{2s}(r_2)g_1(r,r_2)dr_2\right.\right.\\
&\qquad\left.\left.+\int_0^{r_1} u_{2p\to s}(r_2)u_{2p}(r_2)g_1(r,r_2)dr_2\right]\right]\\
&-\frac{2}{9}\frac{u_{1s}(r)}{r}\left[\int_0^\infty \frac{u_{kL}(r_1)u_{2s}(r_1)}{r_1^2}dr_1\int_0^{r_1} u_{1s}(r_2)u_{2s\to p}(r_2)g_1(r,r_2)dr_2\right]\\
&-\frac{2}{3}\frac{u_{2p}(r)}{r}\left[\int_0^\infty \frac{u_{kL}(r_1)u_{2s}(r_1)}{r_1^2}dr_1\left[\int_0^{r_1} u_{2p}(r_2)u_{2s\to p}(r_2)g_0(r,r_2)dr_2\right.\right.\\
&\qquad\left.\left.+\tfrac{6}{25}\int_0^{r_1} u_{2p}(r_2)u_{2s\to p}(r_2)g_2(r,r_2)dr_2\right]\right],
\end{aligned}
$$

$$
\begin{aligned}
I^2_{\mathrm{ep}}(r) = &\frac{2}{5}\frac{u_{2p\to d}(r)}{r}\left[\int_r^\infty \frac{u_{kL}(r_1)u_{2p}(r_1)}{r_1^2}dr_1\right][4\Gamma^0(1s,1s;r)+4\Gamma^0(2s,2s;r)+10\Gamma^0(2p,2p;r)-\tfrac{2}{5}\Gamma^2(2p,2p;r)]\\
&+\frac{4}{15}\frac{u_{2p}(r)}{r}\left[\int_0^\infty \frac{u_{kL}(r_1)u_{2p}(r_1)}{r_1^2}dr_1\right]\\
&\times\left[2\int_0^{r_1} u_{2s\to p}(r_2)u_{2s}(r_2)g_1(r,r_2)dr_2+2\int_0^{r_1} u_{2p\to d}(r_2)u_{2p}(r_2)g_1(r,r_2)dr_2\right.\\
&\left.+\tfrac{14}{5}\int_0^{r_1} u_{2p\to d}(r_2)u_{2p}(r_2)g_1(r,r_2)dr_2-\tfrac{27}{35}\int_0^{r_1} u_{2p\to d}(r_2)u_{2p}(r_2)g_3(r,r_2)dr_2\right]\\
&-\frac{4}{25}\frac{u_{1s}(r)}{r}\left[\int_0^\infty \frac{u_{kL}(r_1)u_{2p}(r_1)}{r_1^2}dr_1\int_0^{r_1} u_{2p\to d}(r_2)u_{1s}(r_2)g_2(r,r_2)dr_2\right]
\end{aligned}
$$

$$-\frac{4}{25}\frac{u_{2s}(r)}{r}\left[\int_0^\infty \frac{u_{kL}(r_1)u_{2p}(r_1)}{r_1^2}dr_1 \int_0^{r_1} u_{2p\to d}(r_2)u_{2s}(r_2)g_2(r,r_2)dr_2\right]$$
$$-\frac{4}{25}\frac{u_{2p\to s}(r)}{r}\left[\int_r^\infty \frac{u_{kL}(r_1)u_{2p}(r_1)}{r_1^2}dr_1\right]\Gamma^2(2p,2p;r)$$
$$-\frac{4}{15}\frac{u_{2s\to p}(r)}{r}\left[\int_r^\infty \frac{u_{kL}(r_1)u_{2p}(r_1)}{r_1^2}dr_1\right]\Gamma^1(2s,2p;r)\ ,$$

where g_λ is given in Eq. (3.31).

APPENDIX B

We give here the explicit expressions of matrix elements M_1, M_2, and M_3 given by Eqs. (4.2), (4.3), and (4.4), respectively:

$$M_1=\frac{1}{\sqrt{3}}\int_0^\infty dr\,u_k(r)u_b(r)r\ ,$$

$$\begin{aligned}M_2=\frac{1}{\sqrt{3}}\Bigg[&\frac{8}{3}\Bigg[\int_0^\infty dr\frac{u_k(r)u_b(r)}{r^2}\int_0^r dr_1 r_1 u_{2s}(r_1)u_{2s\to p}(r_1)\\
&+\int_0^\infty dr\frac{u_k(r)u_b(r)}{r^2}\int_0^r r_1 u_{2p}(r_1)u_{2p\to s}(r_1)dr_1\\
&+2\int_0^\infty dr\frac{u_k(r)u_b(r)}{r^2}\int_0^r r_1 u_{2p}(r_1)u_{2p\to d}(r_1)dr_1\Bigg]\\
&-2\int_0^\infty dr\frac{u_{2p}(r)u_b(r)}{r^2}\int_0^r u_{2p\to s}(r_1)r_1u_k(r_1)dr_1\\
&-\frac{2}{3}\int_0^\infty dr\frac{u_{2s}(r)u_b(r)}{r}\int_0^r u_{2s\to p}(r_1)u_k(r_1)dr_1\\
&+\frac{2}{3}\left[\int_0^\infty u_{2s}(r_2)r_2u_{2p}(r_2)dr_2\right]\left[\int_0^\infty \frac{u_{2p}(r_1)u_b(r_1)}{r_1^2}dr_1\int_0^{r_1} u_{2s\to p}(r_3)u_k(r_3)dr_3\right]\\
&-2\int_0^\infty dr\frac{u_{2p}(r)u_k(r)}{r}\int_0^r u_{2p\to s}(r_1)u_b(r_1)dr_1\\
&-\frac{2}{3}\int_0^\infty dr\frac{u_{2s}(r)u_k(r)}{r^2}\int_0^r r_1u_{2s\to p}(r_1)u_b(r_1)dr_1\\
&+\frac{2}{3}\int_0^\infty r_2u_{1s}(r_2)u_{2p}(r_2)dr_2\int_0^\infty dr\frac{u_k(r)u_{1s}(r)}{r^2}\int_0^r u_{2p\to s}(r_1)u_b(r_1)dr_1\\
&+\frac{2}{3}\int_0^\infty r_2u_{2s}(r_2)u_{2p}(r_2)dr_2\int_0^\infty dr\frac{u_k(r)u_{2s}(r)}{r^2}\int_0^r u_{2p\to s}(r_1)u_b(r_1)dr_1\Bigg]\ ,\end{aligned}$$

$$\begin{aligned}M_3=\frac{1}{\sqrt{3}}\Bigg\{&\frac{8}{3}\Bigg[\int_0^\infty dr\frac{u_k(r)u_b(r)}{r^3}\left[\int_0^r u_{2s\to p}^2(r_1)dr_1+\int_0^r u_{2p\to s}^2(r_1)dr_1+2\int_0^r u_{2p\to d}^2(r_1)dr_1\right]\Bigg]\\
&-\frac{4}{9}\int_0^\infty dr_1\frac{u_{2s}(r_1)u_b(r_1)}{r_1^2}\int_0^{r_1}\frac{u_{2p\to s}(r_2)u_k(r_2)}{r_2^2}dr_2\Bigg[\int_0^{r_1} r_3u_{2s\to p}(r_3)u_{2s}(r_3)dr_3\\
&+2\int_0^{r_1} u_{2p\to s}(r_3)u_{2p}(r_3)r_3dr_3\\
&+4\int_0^{r_1} u_{2p\to d}(r_3)u_{2p}(r_3)r_3dr_3\Bigg]\end{aligned}$$

$$
\begin{aligned}
&-\frac{8}{3}\int_0^\infty dr_2\frac{u_{2p}(r_2)u_b(r_2)}{r_2^2}\int_0^{r_2} dr_1\frac{u_{2p\to s}(r_1)u_k(r_1)}{r_1^2}\left[\int_0^{r_1} u_{2s\to p}(r_3)r_3u_{2s}(r_3)dr_3\right.\\
&\qquad\qquad+\frac{2}{3}\int_0^{r_1} u_{2p\to s}(r_3)r_3u_{2p}(r_3)dr_3\\
&\qquad\qquad\left.+\frac{28}{15}\int_0^{r_1} u_{2p\to d}(r_3)r_3u_{2p}(r_3)dr_3\right]\\
&+\frac{16}{45}\int_0^\infty dr_2\frac{u_{2p}(r_2)u_b(r_2)}{r_2^2}\int_0^{r_2} dr_1\frac{u_{2p\to d}(r_1)u_k(r_1)}{r_1^2}\left[\int_0^{r_1} u_{2p\to s}(r_3)r_3u_{2p}(r_3)dr_3\right.\\
&\qquad\qquad\left.+\frac{3}{5}\int_0^{r_1} u_{2p\to d}(r_3)r_3u_{2p}(r_3)dr_3\right]\\
&-\frac{8}{3}\int_0^\infty dr_1\frac{u_{2p}(r_1)u_k(r_1)}{r_1}\left[\int_0^{r_1} dr_3[u^2_{2s\to p}(r_3)+u^2_{2p\to s}(r_3)]\int_{r_3}^\infty dr_2\frac{u_{2p}(r_2)u_b(r_2)}{r_2^2}\right]\\
&-\frac{728}{75}\int_0^\infty dr_1\frac{u_{2p}(r_1)u_k(r_1)}{r_1}\int_0^{r_1} dr_3u^2_{2p\to d}(r_3)\int_{r_3}^\infty\frac{u_{2p}u_b(r_2)}{r_2^2}dr_2\\
&-\frac{8}{9}\int_0^\infty dr_1\frac{u_{1s}(r_1)u_k(r_1)}{r_1^2}\left[\int_0^{r_1} dr_3[u^2_{2s\to p}(r_3)+u^2_{2p\to s}(r_3)+2u^2_{2p\to d}(r_3)]\right.\\
&\qquad\qquad\left.\times\int_{r_3}^\infty dr_2\frac{u_{1s}(r_2)u_b(r_2)}{r_2}\right]\\
&-\frac{4}{9}\int_0^\infty dr_1\frac{u_{2s}(r_1)u_k(r_1)}{r_1^2}\left[\int_0^{r_1} dr_3[u^2_{2s\to p}(r_3)+2u^2_{2p\to s}(r_3)+4u^2_{2p\to d}(r_3)]\right.\\
&\qquad\qquad\left.\times\int_{r_3}^\infty dr_2\frac{u_{2s}(r_2)u_b(r_2)}{r_2}\right]\\
&+\frac{4}{3}\int_0^\infty dr_1\frac{u_{2s}(r_1)u_k(r_1)}{r_1^2}\int_0^{r_1} dr_3u_{2s\to p}(r_3)u_{2p\to s}(r_3)\int_{r_3}^0\frac{u_{2p}(r_2)u_b(r_2)}{r_2^2}dr_2\Bigg\}.
\end{aligned}
$$

[1]A. Temkin, Phys. Rev. **107**, 1004 (1957).
[2]A. K. Bhatia, A. Temkin, and A. Silver, Phys. Rev. A **12**, 2024 (1975).
[3]R. W. LaBahn and E. A. Garbaty, Phys. Rev. A **9**, 2255 (1974).
[4]R. D. Hudson and V. Carter, J. Opt. Soc. Am. **57**, 651 (1967).
[5]J. J. Chang and H. P. Kelly, Phys. Rev. A **12**, 92 (1975).
[6]A. F. Starace, *Handbuch der Physik,* edited by W. Mehlhorn (Springer, Berlin, 1982), Vol. 31, pp. 1—121.
[7]E. Clementi and C. Roetti, At. Data Nucl. Data Tables **14**, 177 (1974).
[8]A. Temkin, Phys. Rev. **116**, 358 (1959).
[9]R. M. Sternheimer, Phys. Rev. **96**, 961 (1954).
[10]A. K. Bhatia, A. Temkin, A. Silver, and E. C. Sullivan, Phys. Rev. A **18**, 1935 (1978).
[11]L. Lahiri and A. Mukherji, Phys. Rev. **153**, 386 (1966).
[12]R. R. Freeman and D. Kleppner, Phys. Rev. A **14**, 1614 (1976).
[13]R. W. LaBahn, Phys. Lett. **26A**, 326 (1968).
[14]A. Nordsieck, Math. Comput. **16**, 22 (1962).
[15]T. N. Chang, J. Phys. B **8**, 743 (1974).
[16]C. E. Moore, *Atomic Energy Levels,* Natl. Bur. Stand. (U.S.) Circ. No. 467 (U.S. GPO, Washington, D.C., 1971), Vol. 1, p. 89.
[17]P. Risberg, Ark. Fys. **10**, 583 (1956).
[18]M. J. Seaton, Mon. Not. R. Astron. Soc. **118**, 504 (1958).
[19]T. N. Chang and R. T. Poe, Phys. Rev. A **11**, 191 (1975).
[20]K. Butler and C. Mendoza, J. Phys. B **16**, L707 (1983).
[21]M. J. Seaton, Proc. R. Soc. London, Ser. A **208**, 418 (1951).
[22]T. N. Chang (private communication).